Theory of the temperature dependence of the easy axis of magnetization in hcp Gd

Massimiliano Colarieti-Tosti,[1,2,*] Till Burkert,[2] Olle Eriksson,[2] Lars Nordström,[2] and Michael S. S. Brooks[2]

[1]*Department of Physics, Chemistry and Biology, Linköping University, 58183 Linköping, Sweden*
[2]*Department of Physics, Uppsala Universitet, Box 530, 751 21 Uppsala, Sweden*

The magnetic anisotropy energy (MAE) of hcp Gd was calculated from first principles using the full-potential linear muffin-tin orbital method. It was found that the principal contributions to the MAE are the dipole-dipole interaction between the localized $4f$ spins and the spin-orbit interaction of the valence band states. The dipole contribution has the form $\frac{1}{2}K_1^d(1-\cos 2\theta)$, where θ is the angle between the magnetization direction and the c axis. The contribution of the spin-orbit interaction is shown to arise from the polarization of the conduction band that becomes exchange split due to exchange interaction with the localized $4f$ electrons. We argue that this leads to significant contributions from higher order anisotropy constants. An imposed reduced $4f$ moment leads to a repopulation of the electronic states at the Fermi level and a reduced exchange splitting of the valence states, which we demonstrate leads to a modification of the MAE. This modification is in qualitative agreement with the observed temperature dependence of the MAE. In addition, the dependence of the MAE on the c/a ratio has been studied.

PACS number(s): 75.30.Gw, 71.20.Eh, 75.10.Lp

I. INTRODUCTION

The magnetocrystalline anisotropy energy (MAE), $E_A(\theta,\phi)$, is the change in total energy of a ferromagnet when the magnetic moment is rotated through angles θ and ϕ from the crystallographic c and a axes, respectively. The ϕ dependent basal-plane anisotropy is orders of magnitude smaller than the axial anisotropy in hcp Gd and will be neglected here. The MAE of interest is then entirely axial and will be denoted by $E_A(\theta)$. In hcp Gd, according to Ref. 1, the measured value of $E_A(90°)$ is 35 μeV at 4.2 K, with the easy axis of magnetization lying at an angle of 20° from the c axis at low temperature. This is in qualitative agreement with earlier works.[2–6] The preferred orientation of the magnetization is rather surprising since the $4f$ shell is half filled in Gd, leading to a pure spin moment of $7\mu_B$ and to a $4f$ shell charge distribution that is expected to be spherical. The sphericity of the $4f$ shell is indirectly confirmed by the fact that the MAE of Gd is two orders of magnitude smaller than that of the other $4f$ metals, where the principal contribution to the MAE comes from the interaction between the crystalline electric field (CEF) and the electric multipole moments of the $4f$ charge cloud.[7] If Gd is considered to be in a pure S state the electric multipole moments are zero and there is no CEF contribution to the MAE. Of course, a small deviation from an S state could still be compatible with the order of magnitude of the MAE, but a theoretical calculation[8] showed that the MAE calculated assuming an S state for Gd is consistent with experimental studies. Single ion contributions originating from the nonsphericity of the $4f$ shell of Gd induced by spin-orbit coupling must therefore be of negligible magnitude. In a previous Letter,[8] and in the remainder of this paper, we give additional arguments that deviations from an S state are not necessary in order to explain the observed MAE of hcp Gd. In our proposed model the origin of the MAE of Gd at low temperature is the sum of the magnetic anisotropy energy due to the spin-orbit splitting of the band electrons and the dipole-dipole interaction between the large localized $4f$ spin moments.

The remainder of this paper is organized as follows. In Sec. II we report our most accurate calculations of $E_A(\theta)$. Then, in Sec. III, we review the measurements of the temperature dependence and sketch our strategy for trying to tackle this problem using zero-temperature calculations. The calculated dependence of the MAE upon a reduced $4f$ moment, designed to simulate the reduction of the magnetic moment with temperature, is discussed in Sec. III A. In Sec. III B, we describe the effect on the MAE of summing the eigenvalues with a Fermi-Dirac distribution function to simulate the temperature dependent occupancy of the electronic states in the vicinity of the Fermi surface. Finally, the dependence of the MAE upon the c/a ratio is discussed in Sec. III C.

II. LOW-TEMPERATURE MAGNETOCRYSTALLINE ANISOTROPY

In Ref. 8 we proposed that the two main contributions to the MAE of hcp Gd are the dipole-dipole interaction between the large $4f$ spins and the magnetic anisotropy due to the conduction electrons. The dipole-dipole interaction between the large localized spins makes a significant contribution of the form $E_A^d=\frac{1}{2}K_1^d(1-\cos 2\theta)$,[9,10] with K_1^d calculated by lattice sums[11] to be equal to 7.5 μeV. The conduction electron magnetic anisotropy is due to the spin-orbit interaction of the itinerant electrons, which is known to be small in the $3d$ transition metals.[12–14] The spin-orbit parameter is about 0.05 eV for the $3d$ states in Fe, leading to a spin-orbit splitting of about 0.13 eV. A considerably larger MAE is found in magnetic actinide compounds, in which the main contribution arises from the spin-orbit interaction of the $5f$ states. The $5f$ spin-orbit parameter for U is about 0.2 eV, leading to a spin-orbit splitting of the $5f$ states of about 0.7 eV.[15,16] The rare earth metals are in an intermediate situation. The spin-
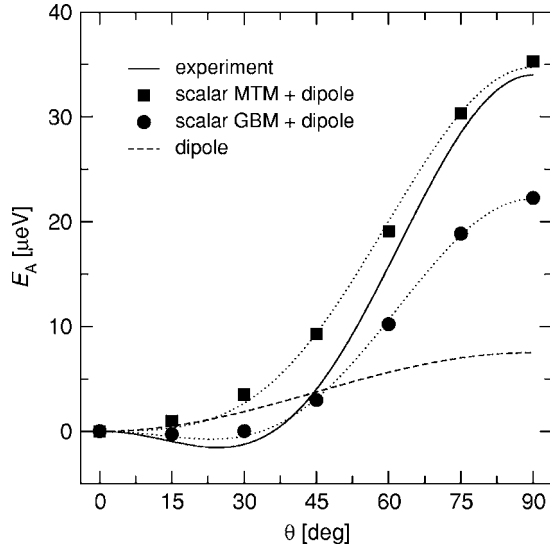
FIG. 1. Calculated MAE of hcp Gd as a function of the angle θ from the c axis. The full line is the experimental data from Ref. 1. The symbols are the total MAE, i.e., the dipole contribution plus the conduction band contribution, obtained using the MTM (squares) and the GBM (circles, from Ref. 8) for the calculation of the scalar-relativistic potential. The MAE was in both cases calculated with the force theorem using the MTM. The dotted lines are fits of Eq. (1) to the calculated results, and the dashed line is the dipole contribution alone.

orbit parameter for the $5d$ states in the rare-earth metals is about 0.1 eV, leading to a spin-orbit splitting of about 0.4 eV. The $5d$ states are more than 10 eV broad and would not by themselves be magnetic. However, the exchange interaction with the $4f$ states polarizes them and the conduction electron magnetic moment reaches a maximum value for Gd of $0.63\mu_B$/atom.[17]

We note here that there has been a lively debate concerning whether the Gd $4f$ states should be treated as localized core states or should be allowed to hybridize as band states.[18–23] We have given arguments for treating the $4f$ states as localized core states in Ref. 8 and this is the approximation we have used throughout this work.

Our model for the origin of the MAE is as follows. An applied magnetic field interacts with and orients both $4f$ and conduction electron magnetic moments. The exchange field of the $4f$ spin is much larger than any applied field and it will force the conduction electron moment to be parallel to the $4f$ moment. Although the MAE is mainly due to the spin-orbit interaction of the conduction electrons, an applied field couples to the $4f$ spin, and therefore the MAE appears to be intrinsic to the localized $4f$ states if they are described by a spin Hamiltonian. With this model it is possible to obtain an easy axis of magnetization lying in a direction that is not parallel to a crystal symmetry axis without requiring any deviation from a $4f$ shell S state.

The results obtained from the above described model are summarized in Fig. 1. The sum of the calculated band electron anisotropy and the dipole-dipole interaction are plotted together with the experimental data. The latter is derived from the regular part of the magnetic torque as defined in Eq.

(4) of Ref. 1. The irregular part of the magnetic torque shifts the minimum in $E_A(\theta)$ to 20° away from the c axis. The calculations were made for the low temperature lattice constants, $a=3.62$ Å and $c/a=1.6$.[24]

All calculations presented here were made with a fully relativistic implementation of the full-potential linear muffin-tin orbital method (FP-LMTO).[25] The conduction band basis set included a double basis set of $5s$, $5p$, $6s$, $6p$, and $5d$ states. For the evaluation of the band electron anisotropy we have made use of fully self-consistent calculations as well as the force theorem.[26] For the latter we first calculated, self-consistently, a scalar-relativistic potential, i.e., without the spin-orbit interaction, within the local spin density approximation (LSDA).[27] Then we calculated the eigenvalues with the spin-orbit interaction for a given spin quantization axis using the self-consistent potential. The MAE was then approximated as the difference of the eigenvalue sums for a given angle and that for $\theta=0°$. For the MAE calculations presented in Fig. 1 the angles of the quantization axis were 0°, 15°, 30°, 45°, 60°, 75°, and 90° off the c axis. Then the parameters A and B in the expansion of the MAE,

$$E_A(\theta) = A(\cos 2\theta - 1) + B(\cos 4\theta - 1), \tag{1}$$

were obtained from a fit to the calculated $E_A(\theta)$. For the calculations presented in subsequent sections, $E_A(\theta)$ was calculated for the angles 30° and 90° only, and the expansion coefficients A and B were evaluated from

$$A = -\frac{1}{2}E_A(90°),$$

$$B = -\frac{2}{3}E_A(30°) + \frac{1}{6}E_A(90°). \tag{2}$$

For the calculations presented in Fig. 1 this latter procedure yields $A=-17.67$ μeV and $B=3.55$ μeV, which should be compared to $A=-17.36$ μeV and $B=4.00$ μeV obtained from a fit of Eq. (1). The small difference between these two sets of anisotropy constants is not unexpected for such tiny quantities. We want to show here that substantial values for higher-order anisotropy constants can be present in an S-state system, which is valid for both sets of A and B. Indeed, the difference itself is an indirect proof that higher order anisotropy constants are of importance. It is not feasible to calculate the MAE of Gd to the last μeV of accuracy, therefore, for computational efficiency, in the remainder of this paper, we have evaluated the coefficients A and B from Eq. (2).

The easy axis of magnetization is obtained by minimizing the MAE in Eq. (1) with respect to the angle θ, which yields

$$\theta_m = \frac{1}{2}\arccos\left(-\frac{A}{4B}\right), \tag{3}$$

in terms of the expansion coefficients A and B. Thus, a criterion for the occurrence of an easy axis of magnetization not pointing along the c axis is

$$4B > -A \geqslant 0, \tag{4}$$

or, in terms of the calculated values for $E_A(30°)$ and $E_A(90°)$,

$$16E_A(30°) < E_A(90°) \text{ and } E_A(90°) \geqslant 0. \qquad (5)$$

For the present calculations the modified tetrahedron method[28] (MTM) was used throughout the whole procedure for calculating the MAE, i.e., both for the calculation of the self-consistent scalar potential as well as for the force theorem[26] calculations. This is in contrast to Ref. 8 where the Gaussian broadening method[29] (GBM) was used to calculate the self-consistent potential and the MAE was evaluated from the force theorem using the MTM. We will refer to these two calculations as the MTM and the GBM results, respectively. Note that the MTM was used for the force theorem step in both cases.

The overall behavior of $E_A(\theta)$ is very well reproduced by the MTM calculations. However, the presently calculated MAE of hcp Gd, plotted in Fig. 1, shows no minimum in $E_A(\theta)$ at an angle of 20°, in contrast to what was previously reported[8] and redrawn also in Fig. 1. Furthermore, the value for $E_A(90°)$ calculated by operating the force theorem step on a GBM potential is about 40% smaller than the one obtained when also the scalar potential is calculated with the MTM. The observed dependence of the calculated MAE to the details of the BZ sampling of the scalar-relativistic calculation is rather surprising, but is consistent with the picture described in Ref. 1 of a strong dependence of the MAE of Gd upon the detailed structure of the Fermi surface. The charge and the magnetization densities that are obtained from the GBM differ slightly from those that are calculated with the MTM. The GBM results in a conduction band polarization of $0.743\mu_B$, which is smaller than that obtained from the MTM, $0.765\mu_B$. This tiny change of the the 5d moment is enough to restore an easy axis off the c axis, as will be discussed in Sec. III A, where it will be shown that the calculated easy axis is extremely dependent on the value of the valence band moment. An energy minimum away from the c axis is also restored if a reduced moment of $6.95\mu_B$ is used for the 4f shell. Note that this cannot be interpreted as a deviation from an S state, since the 4f shell is always considered as spherical in our calculations, only its moment is changed. The main effect of the reduced 4f moment is to change the polarization of the valence electrons, which are responsible for the occurrence of a minimum in $E_A(\theta)$, resulting in an easy axis direction that is not parallel to the c axis. The other effect is a small reduction of the dipole anisotropy, which scales quadratically with the reduced moment. In fact, in our model for the evaluation of the MAE for any value of the 4f moment all contributions to the MAE from the interaction between the 4f charge cloud and the CEF are excluded since we assume a Russel-Saunders coupling for the 4f shell of Gd.

Since the MAE is sensitively dependent on the correct sampling of the BZ, a test of the convergence of the valence band contribution to E_A which we refer to as E_A^{band}, with respect to the number of k points is appropriate. In Fig. 2 the results for $E_A^{band}(30°)$ and $E_A^{band}(90°)$, calculated with the force theorem for different samplings of the BZ, are shown. The self-consistent potential used for these calculations, and all other calculations presented here, was calculated with $2 \times 10^4 k$ points in the full BZ.

The values for $E_A^{band}(30°)$ in Fig. 2 were multiplied by a factor of 16, to illustrate how sensitive the occurrence of an
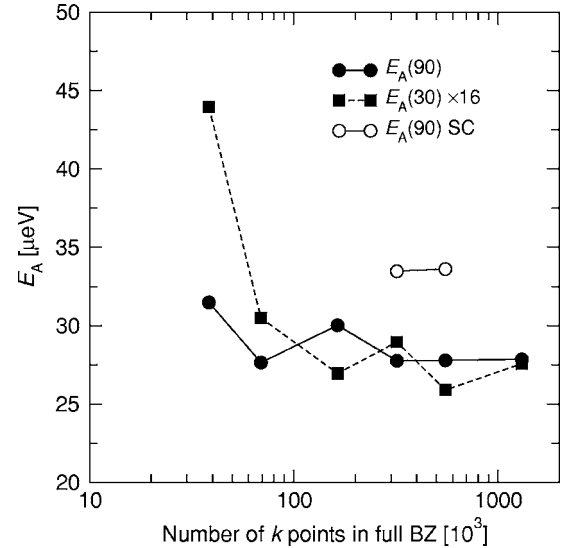

FIG. 2. Convergence of the valence electron MAE with respect to the number of k points in the full BZ. The closed symbols are the results obtained with the force theorem and the open circles present the results from self-consistent calculations. The values for $E_A^{band}(30°)$ are scaled by a factor 16 to reflect the criterion for the occurrence of an easy axis off the c axis, Eq. (5).

easy axis of magnetization away from the c axis is on the BZ sampling. Whereas the values for $E_A^{band}(90°)$ can be considered converged with respect to the number of k points, this is not quite the case for $E_A^{band}(30°)$, even with the largest set used, containing $1.3 \times 10^6 k$ points. The fact that $E_A^{band}(30°)$ is converging slower and is also about 16 times smaller than $E_A^{band}(90°)$ leads to a situation where the occurrence of an easy axis not parallel to the c axis is dependent on the used k point set, as can be seen in Fig. 2. For all results reported below, and those shown in Fig. 1, the k point set of Fig. 2 corresponding to $5.5 \times 10^5 k$ points was used for the force theorem calculations.

To test the applicability of the force theorem in the present case we also performed a self-consistent calculation of $E_A(90°)$. The obtained value is 20% larger than that obtained from the force theorem, an agreement that can be considered to be sufficient, given the small values of the MAE. Let us point out once more that, in this work, we want to investigate whether or not in an S-state model of Gd the anisotropy constant B of Eq. (1) is non-negligible as compared to A. This fact remains true even if A is increased by 20% as the self-consistent calculation would suggest.

III. TEMPERATURE DEPENDENCE OF THE EASY AXIS OF MAGNETIZATION

The measured temperature dependence of the easy axis of magnetization of hcp Gd is redrawn in Fig. 3 and is seen to be highly unusual. Although not entirely consistent, all measurements show that, starting from an angle of about 30° away from the c axis at low temperature, the easy axis moves towards the basal plane with increasing temperature, and then back towards the c axis before the Curie temperature is
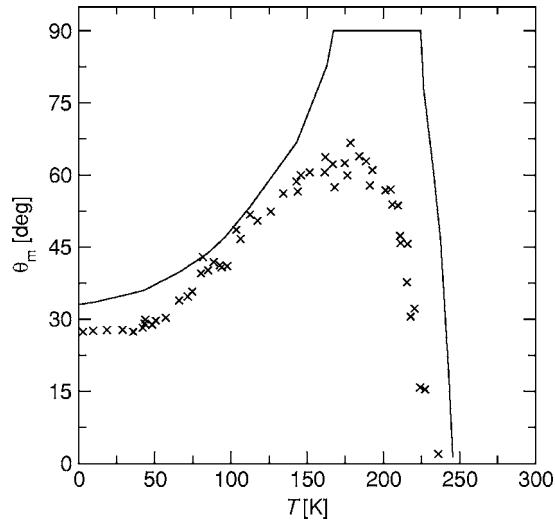
FIG. 3. Measured temperature dependence of the easy axis of magnetization of hcp Gd. The full line is the data from Ref. 2, while the crosses show the data from Refs. 6 and 30.

reached. Smith *et al.*,[4,5] with magnetic torque measurements, and Cable and Wollan,[6] with neutron diffraction measurements, report a maximum angle off the *c* axis of about 60° at a temperature close to 190 K, while Graham[2,3] claimed that the easy axis lies in the basal plane between 170 K and 233 K. All these authors found that the easy axis at low temperature is at about 30° and that, above 240 K[4–6] or 250 K,[2,3] respectively, the easy axis is the *c* axis. Note that the most recent measurements[1] give a value of 20° for the low temperature easy axis of magnetization.

Our first attempt to gain some insight into the mechanism responsible for the unusual temperature dependence of the easy axis was to examine the temperature dependence of the MAE expanded in terms of the anisotropy constants K_n,

$$E_A(\theta,\phi) = K_1 \sin^2\theta + K_2 \sin^4\theta + (K_3 + K_4 \cos 6\phi)\sin^6\theta,$$

$$(6)$$

with the low-temperature measured values of K_n scaled by the magnetization power laws derived from spin wave theory.[10] This attempt failed already at very low temperature. We suggest that the main reason for the discrepancy is that spin wave theory alone does not apply to this case. As was discussed in Ref. 8, the fine structure of the electronic energy levels close to the Fermi surface is important for determining the low temperature behavior, and it is reasonable to assume that this is also the case at higher temperatures. This cannot be captured by spin wave theory which attributes the decrease of the MAE with temperature to thermal population of spin wave states.

Temperature has many effects on the MAE. The most obvious one is to reduce the magnetization;[31] another is to change the structure and is manifested mainly in a change of the *c/a* ratio.[24] Both of these effects may be simulated in first-principles calculations since both the magnitude of the localized 4*f* magnetic moment and the *c/a* ratio are an input to the self-consistent calculations (the conduction electron

moment is calculated self-consistently for any given 4*f* magnetic moment). A change of the eigenvalues and a redistribution of the populated levels close to the Fermi energy must also occur. In order to try to capture the change in the electronic structure with increasing temperature the simplest feasible approach is to use a Fermi-Dirac distribution function to calculate the occupancy of the electronic states close to the Fermi surface. Any change of the levels themselves with temperature is neglected in this approach. In the following we address the effect of a reduced magnetization, the repopulation of the electronic states at the Fermi surface, and the *c/a* ratio separately.

A. Reduced magnetization

We have evaluated the total MAE, i.e., the sum of the dipole contribution and that from the conduction electrons, with a constrained 4*f* moment m_{4f} of 6.95, 6.8, 6.6, 6.4, 6, 5, 4, 3, 2, and 1.5μ_B, yielding conduction band polarizations of 0.762, 0.754, 0.744, 0.734, 0.715, 0.664, 0.600, 0.475, 0.337, and 0.260μ_B, respectively. The results for the expansion coefficients A and B, defined in Eq. (1), and the easy axis of magnetization, calculated from Eq. (3), are plotted in Fig. 4. Also, we present the data for θ_m (lower part of Fig. 4) again in Fig. 6 as a function of temperature. The latter was obtained by comparing the calculated magnetic moment to the measured magnetization as a function of temperature.[31] This is a very rough estimation, since the local moments are not trivially coupled to the measured magnetization, especially at the higher temperatures.

We find that the easy axis, which lies along the *c* axis for the full moment case, moves towards the basal plane with decreasing 4*f* moment. Already for a conduction band moment of 0.762μ_B (m_{4f}=6.95μ_B) we obtain an easy axis angle of 17°. When the moment is further reduced to 0.754μ_B (m_{4f}=6.8μ_B) the angle increases to 35°. The maximum angle off the *c* axis reaches about 50° for a conduction band moment of 0.744μ_B, corresponding to a constrained 4*f* moment of 6.6μ_B. The calculated easy axis flips back to the *c* axis when the conduction band moment is further reduced to 0.734μ_B (m_{4f}=6.4μ_B) and remains on this axis for all lower values of the magnetization. This behavior is in qualitative agreement with the observed temperature dependence of the easy axis plotted in Fig. 3. However, experimentally[4–6] it was found that the easy axis reaches its maximum value at a temperature of around 180 K, while in our simple calculations this happens already at 80 K. Also, the flipping back to the *c* axis occurs experimentally at a temperature close to the Curie temperature of Gd, while our simple model predicts this to occur at a temperature of 100 K. Nevertheless, the qualitative agreement between the calculated and measured temperature dependence of the easy axis is satisfactory given that our calculations are necessarily approximate. In particular one has to note that collective excitations such as spin waves are beyond the reach of this simple analysis. The behavior of the easy axis is readily explained by inspection of the behavior of *A* and *B* shown in the upper part of Fig. 4. The only regions in which the criterion stated in Eq. (4) is
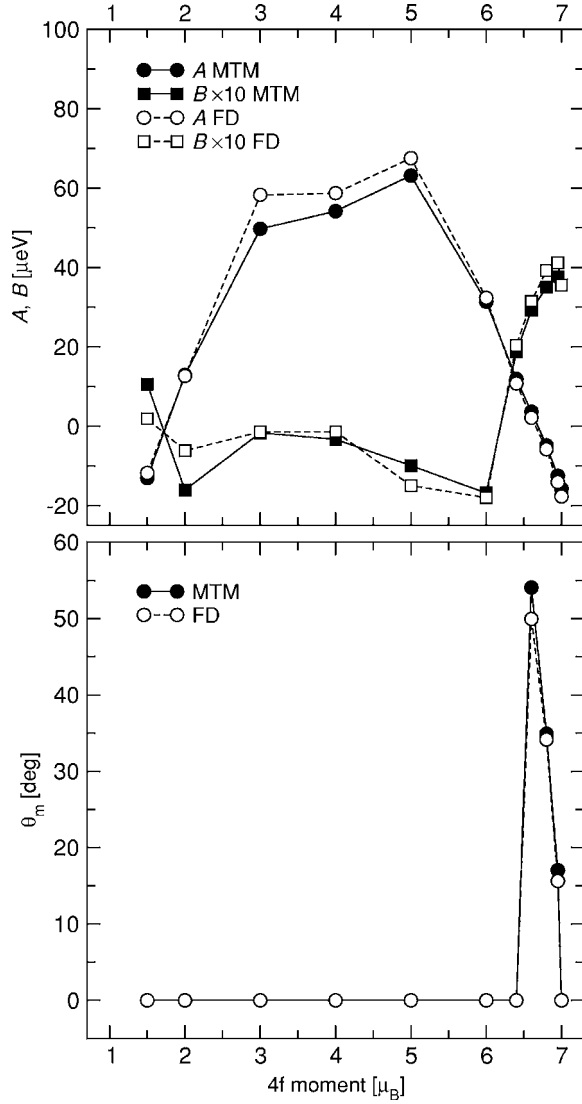
FIG. 4. Expansion coefficients A and B for $E_A(\theta)$ (upper) and easy axis of magnetization θ_m (lower) as a function of the reduced moment for the $4f$ shell. The results obtained with the MTM are marked by filled symbols, whereas the results calculated with the Fermi-Dirac (FD) distribution (cf. Sec. III B) are marked by open symbols. Note that B is enlarged by a factor of 10.

fulfilled are in the vicinity of the full moment of $7\mu_B$ or close to the reduced $4f$ moment of $1.5\mu_B$. In this latter case, though, our approach is of questionable validity and its prediction cannot be trusted. The strong dependence of the easy axis of magnetization on the reduced $4f$ moment illustrates once more how important the correct description of the electronic structure is for the calculation of the MAE. Since the calculated conduction band moment of $0.76\mu_B$ is slightly larger than the experimentally observed moment, an entirely correct description of the MAE cannot be expected. Finally, it is worth noting that the overall size of the MAE, $E_A(90°)=-2A$, does not simply become smaller as the $4f$ moment is reduced, as can be seen from Fig. 4.

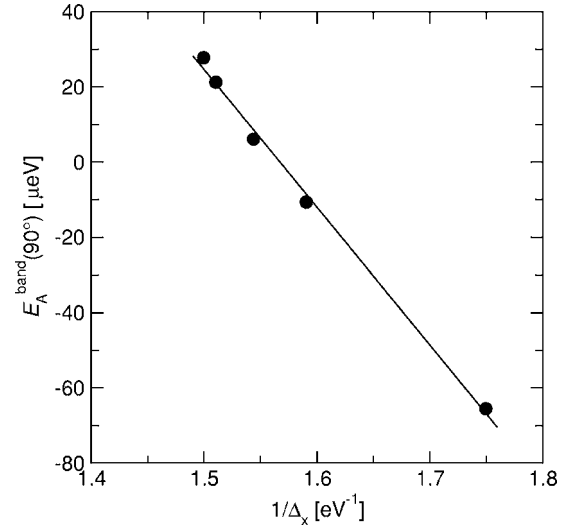We also analyzed the change of the MAE by perturbation theory[14,32] for the values of the reduced $4f$ moment between

FIG. 5. $E_A^{\text{band}}(90°)$ plotted against the inverse of $\Delta_x = m_{4f}I_{4f,5d} + m_{5d}I_{5d,5d}$, as described in the text ($1/\Delta_x = 1.5$ eV^{-1} for the $4f$ full moment and 1.75 eV^{-1} for $m_{4f}=6$). Closed circles are calculated values while the line is a linear regression of the former.

$7\mu_B$ and $6\mu_B$. For a uniaxial MAE the expression is of the form

$$E_A^{\text{band}}(90°) \approx \sum_{o,u} \frac{|\langle o|H_{\text{so}}|u\rangle|^2}{\epsilon_o - \epsilon_u}, \qquad (7)$$

where o and u represent the occupied and unoccupied states, respectively, H_{so} is the spin-orbit matrix element, and ϵ_o and ϵ_u are the eigenvalues of the scalar-relativistic Hamiltonian. If one assumes that most of the states that are coupled by H_{so} are due to bands that are degenerate in the limit of a vanishing valence band moment, one can approximate $\epsilon_o - \epsilon_u$ by the valence band exchange splitting Δ_x. Since most of the valence band moment is located on the $5d$ orbitals, one may approximately write $\Delta_x = m_{5d}I_{5d,5d} + m_{4f}I_{5d,4f}$, where $I_{l,l'}$ is the exchange interaction between orbitals l and l' and m_{4f} and m_{5d} are the reduced $4f$ moment and the induced $5d$ moment, respectively. From Eq. (7) it becomes clear that $E_A^{\text{band}}(90°)$ should be inversely proportional to Δ_x. In Fig. 5, using values for $I_{5d,5d}$ and $I_{5d,4f}$ from Ref. 33, it is shown that this is indeed the case.

Note that the lowest-order nonvanishing anisotropy constant, A in Eq. (1), is not enough to predict the interesting behavior of $E_A^{\text{band}}(\theta)$, i.e., the occurrence of an easy axis of magnetization off the c axis. Extending the perturbation theory to higher order involves higher powers of the ratio of the matrix elements $\langle o|H_{\text{so}}|u\rangle$ and the exchange interaction Δ_x, corresponding to higher order anisotropy constants. This ratio is a good expansion parameter for transition metals where the exchange band splitting is considerably larger than the spin-orbit splitting. In Gd these quantities are of comparable size, and the expansion has a slower convergence. Hence, higher order anisotropy constants make a significant contribution to the MAE of hcp Gd.
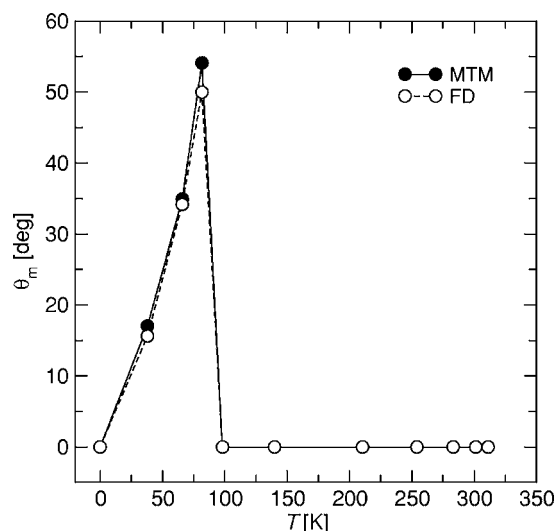
FIG. 6. Easy axis of magnetization as a function of the temperature (see text). The results obtained with the MTM are marked by filled symbols, whereas the results calculated with the Fermi-Dirac (FD) distribution (cf. Sec. III B) are marked by open symbols. Note that the calculation denoted FD also includes a reduction of the 4f moment with temperature (see text).

B. BZ sampling using a Fermi-Dirac distribution

If one assumes that the electronic structure of a solid is not modified by a temperature change, the only effect that temperature has on the eigenvalue sum, and hence the MAE, is a change of the occupancy of the energy levels near the Fermi surface. This redistribution is determined by the Fermi-Dirac distribution function. In reality, especially at high temperature, the change in the band structure can be substantial as can be the effects of collective magnetic excitations such as spin waves. The following analysis attempts to isolate the effect of a finite temperature Fermi-Dirac distribution whereas other effects of temperature are neglected.

We used the measured magnetization as a function of temperature of Ref. 31 in order to assign a temperature to each reduced moment calculation presented in the previous section. Then we recalculated the sum of the eigenvalues for each value of the 4f moment using a Fermi-Dirac distribution for the corresponding temperature. The constants A and B evaluated in this way and the easy axis of magnetization θ_m are shown in Figs. 4 and 6, together with the results obtained from the MTM described in the previous section. It can be seen that a Fermi-Dirac distribution with a finite temperature changes A and B and the easy axis of magnetization only marginally. Thus, the repopulation of the electronic states at the Fermi surface has a negligible influence on the temperature dependence of the easy axis of magnetization for hcp Gd.

C. Dependence of the MAE on *c/a*

We have in addition calculated the MAE of hcp Gd with c/a ratios of 1.57, 1.59, 1.61, $\sqrt{8/3}$, and 1.67, using a constant volume equal to the experimental low temperature one.[24] The results for the expansion coefficients A and B
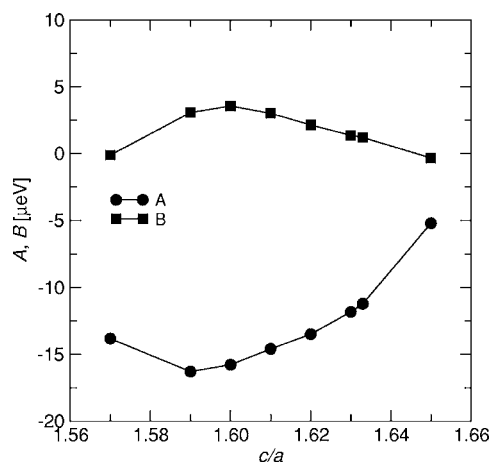

FIG. 7. Expansion coefficients A and B for $E_A(\theta)$, as defined in Eq. (1), as a function of the c/a ratio.

[cf. Eq. (1)] for the total MAE, i.e., the dipole contribution plus that from the conduction electrons, are reported in Fig. 7. It can be seen that the MAE does not depend monotonically upon the c/a ratio. Note that the dipole-dipole contribution alone depends linearly on the c/a ratio, favoring the c or a axis depending on whether the ratio is less than or greater than approximately $\sqrt{8/3}$, respectively. We emphasize that the dipole-dipole contribution can only have either the c axis or the basal plane as an easy axis of magnetization. The calculated easy axis does not deviate from the c axis as a function of the c/a ratio, as can be deduced from Fig. 7 and Eq. (4).

Concerning the temperature dependence of the easy axis, according to Darnell,[24] the c/a of Gd undergoes a conspicuous change in the temperature range between 200 K and 300 K. In this temperature range the lattice constant a is found to follow a normal thermal expansion while c shrinks with about 0.25% from its initial value. Thus one expects a change of c/a as large as 0.3–0.4 % in this temperature range. This means that only the $E_A(\theta)$ curves for c/a equal to 1.6 and to 1.59 are relevant to our problem. These curves are very similar to each other (cf. Fig. 7), and the difference between them is almost entirely due to the difference in the dipole contribution. The latter becomes smaller as the temperature increases, so that the high temperature anisotropy for $c/a=1.59$ will be very close to the one for 1.6. Therefore we believe that the temperature induced change of the c/a ratio is not a determining factor for the observed temperature dependence of the easy axis. However, the possibility of modifying the MAE of Gd by changing the c/a ratio might be explored experimentally.

IV. CONCLUSIONS

The magnetic anisotropy energy of hcp Gd at low temperature was calculated from first principles, obtaining good agreement with the most recent experimental data. It was shown that the dipole-dipole interaction between the large spins of the localized 4f shell and the spin-orbit splitting of the itinerant band electrons are the two major contributions

to the observed MAE. No deviation from the S state for the $4f$ shell is necessary in order to account for the MAE or to explain the measured easy axis of magnetization at low temperature. The applicability of the force theorem to the present case was tested with self-consistent calculations, and our results suggest that the force theorem is sufficiently accurate to evaluate the MAE of hcp Gd.

In order to shed some light on the remarkable temperature dependence of the easy axis of magnetization we also calculated $E_A(\theta)$ as a function of the magnetic moment by constraining the $4f$ spin moment. This was done in an attempt to simulate the effect of the temperature induced reduction of the magnetization, in particular the valence band moments. We found that the nontrivial behavior of the easy axis upon the $4f$ moment is similar to the experimental trend that is observed with increasing temperature. The calculated easy axis is on the c axis for the full moment. Decreasing the constrained moment, i.e., increasing the temperature, the angle increases until the easy axis reaches a maximum value of about 50°. Then the calculated easy axis starts to turn back towards the c axis, which is again the easy axis of magnetization at a temperature estimated to be around 100 K, in qualitative agreement with the experimental findings. The influence of the c/a ratio on $E_A(\theta)$ was investigated, and it was found that this structural parameter can be used to modify the overall size and maybe also the angular behavior of the MAE of Gd. We propose that this could be examined experimentally.

Our analysis leads to the conclusion that the principal reason for the unusual temperature dependence of the easy axis is the dependence of the band electron contribution to the magnetic anisotropy energy upon the induced magnetic moment and, therefore, temperature. Both the change in c/a ratio and the redistribution of the population of levels close to the Fermi surface, as a function of temperature, have less of an effect upon the temperature dependence of the easy axis. The strong dependence of the easy axis of magnetization on the details of the BZ sampling and on the reduced $4f$ moment illustrates how important the correct description of the electronic structure, and hence the Fermi surface, is for the calculation of the MAE.

Finally, let us note that the mechanism we hold responsible for the MAE of Gd is present in the entire rare-earth series. The only difference is that in the other rare-earth metals the contribution to the MAE originating from interactions of the nonspherical part of the $4f$ shell with the CEF is two orders of magnitude larger and therefore completely dominates the magnetic anisotropy. Our calculations of the MAE of Gd with a reduced $4f$ moment constitutes an estimate of the valence band anisotropy contribution to the MAE in the rare-earth series.

*Electronic address: mamo@ifm.liu.se

[1] J. J. M. Franse and R. Gersdorf, Phys. Rev. Lett. **45**, 50 (1980).

[2] J. C. D. Graham, J. Phys. Soc. Jpn. **17**, 1310 (1962).

[3] J. C. D. Graham, J. Appl. Phys. **34**, 1341 (1963).

[4] R. L. Smith, W. D. Corner, B. K. Tanner, R. G. Jordan, and D. W. Jones, *Rare Earths and Actinides 1977* (IOP, Bristol, 1978), p. 215.

[5] R. L. Smith, B. K. Tanner, and W. D. Corner, J. Phys. F: Met. Phys. **7**, L229 (1977).

[6] J. W. Cable and E. O. Wollan, Phys. Rev. **165**, 733 (1968).

[7] R. J. Elliott, in *Magnetic Poperties of Rare Earth Metals* (Plenum Press, London, 1972), Chap. 1.

[8] M. Colarieti-Tosti, S. I. Simak, R. Ahuja, L. Nordström, O. Eriksson, D. Åberg, S. Edvardsson, and M. S. S. Brooks, Phys. Rev. Lett. **91**, 157201 (2003).

[9] J. Jensen and A. R. Mackintosh, *Rare Earth Magnetism* (Clarendon Press, Oxford, 1991).

[10] M. S. S. Brooks and D. A. Goodings, J. Appl. Phys. **39**, 1340 (1968).

[11] J. M. Ziman, *Principles of the Theory of Solids* (Cambridge University Press, Cambridge, UK, 1979).

[12] G. H. O. Daalderop, P. J. Kelly, and M. F. H. Schuurmans, Phys. Rev. B **41**, 11919 (1990).

[13] J. Trygg, B. Johansson, O. Eriksson, and J. M. Wills, Phys. Rev. Lett. **75**, 2871 (1995).

[14] P. Bruno, *Magnetismus von Festkörpern und Grenzflächen* (Forschungszentrum Jülich, Jülich, 1993), Chap. 24.

[15] M. S. S. Brooks, B. Johansson, O. Eriksson, and H. Skriver, Physica B & C **144**, 1 (1986).

[16] G. H. Lander, M. S. S. Brooks, B. Lebech, P. J. Brown, O. Vogt, and K. Mattenberger, J. Appl. Phys. **69**, 4803 (1991).

[17] L. W. Roeland, G. J. Cock, F. A. Muller, A. C. Moleman, K. A. McEwen, R. G. Jordan, and D. W. Jones, J. Phys. F: Met. Phys. **5**, L233 (1975).

[18] J. O. Dimmock and A. J. Freeman, Phys. Rev. Lett. **13**, 750 (1964).

[19] B. N. Harmon, J. Phys. Colloq. **40**, C5/65 (1979).

[20] B. Kim, A. B. Andrews, J. L. Erskine, K. J. Kim, and B. N. Harmon, Phys. Rev. Lett. **68**, 1931 (1991).

[21] D. J. Singh, Phys. Rev. B **44**, 7451 (1991).

[22] D. M. Bylander and L. Kleinman, Phys. Rev. B **49**, 1608 (1994).

[23] M. S. S. Brooks and B. Johansson, in *Handbook of Magnetic Materials*, edited by K. Buschow (North-Holland, Amsterdam, 1993), Vol. 7.

[24] F. J. Darnell, Phys. Rev. **130**, 1825 (1963).

[25] J. M. Wills, O. Eriksson, M. Alouani, and D. L. Price, in *Electronic Structure and Physical Properties of Solids: The Uses of the LMTO Method* (Springer, Berlin, 2000), pp. 148–167.

[26] M. Weinert, R. E. Watson, and J. W. Davenport, Phys. Rev. B **32**, 2115 (1985).

[27] U. von Barth and L. Hedin, J. Phys. C **5**, 1629 (1972).

[28] P. E. Blöchl, O. Jepsen, and O. K. Andersen, Phys. Rev. B **49**, 16223 (1994).

[29] M. Methfessel and A. T. Paxton, Phys. Rev. B **40**, 3616 (1989).

[30] W. D. Corner and B. K. Tanner, J. Phys. C **9**, 627 (1975).

[31] H. E. Nigh, S. Legvold, and F. H. Spedding, Phys. Rev. **132**, 1092 (1963).

[32] P. Bruno, Phys. Rev. B **39**, R865 (1989).

[33] M. S. S. Brooks, O. Eriksson, and B. Johansson, J. Phys.: Condens. Matter **1**, 5861 (1989).